

# A Numerical and Experimental Investigation into the Effect of Welding Parameters on Thermal History in Friction Stir Welded Copper Sheets

A. Alavi Nia\*, A. Shirazi

Mechanical Engineering Department, Bu-Ali Sina University, Hamedan, Iran.

## Article info

### Article history:

Received 09 January 2017

Received in revised form

23 February 2017

Accepted 30 May 2017

### Keywords:

Friction stir welding

Finite element

Copper

Thermal history

Welding parameters

## Abstract

One of the important issues in the process of Friction Stir Welding (FSW) is to determine the thermal history and its distribution in the work piece during the welding process. Several analytical and empirical relations have been suggested to estimate the amount of heat transferred to the work piece; one of the relations is Frigaad relation. In the present study, thermal history was determined for joined parts of copper sheets under various welding conditions by Frigaad relation and numerical method. Furthermore, results were compared with the experimental results which had a good agreement with numerical results. In addition, the thermal field was also determined for any welding conditions and at any given moment. By conducting this study, it is evident that the traverse velocity change mainly affects the amount of transferred heat and change in rotational speed dramatically changes the temperature of the process.

## Nomenclature

$A$	Area of the format channel moistened by water	$\dot{q}$	Rate of heat transferred to the cooling water
$h$	Convective heat transfer coefficient	$\dot{m}$	Cooling water mass rate
$N$	Rotational speed	$P$	Pressure
$\dot{q}$	Rate of net heat input	$c$	Heat capacity
$\dot{q}_{\text{net}}$	Net heat transferred to the workpiece	$R$	Tool radius
$T$	Temperature	$v$	Traverse speed
$\mu$	Dynamic friction coefficient	$w$	Angular speed

## 1. Introduction

Friction Stir Welding (FSW), as a solid state joining process, is widely utilized to weld various materials that are difficult to fusion weld. This method was originally invented for connecting aluminum parts but its usage was quickly extended to other materials such as magnesium, copper, steel, titanium, nickel alloys [1] and many polymeric [2] and thermoplastic [3] materi-

als. It can be used to connect pieces of different materials as well [4-6]. The method was invented and introduced by The Welding Institute (TWI) in England in 1991 [7].

Recently, by expanding the application of copper and its alloys as a structural material, the demand for this method of welding has grown [8], accordingly copper was chosen for the present study. One of the significant issues in FSW is to determine the thermal

\*Corresponding author: A. Alavi Nia (Professor)

E-mail address: alavi1338@yahoo.com

<http://dx.doi.org/10.22084/jrstan.2017.12687.1016>

ISSN: 2588-2597

**Table 1**

The material properties of concrete specimens.

Cu	Ag	Be	Co	Cr	Si	Ni	Fe	Al	Mn	P	Sn	Pb	Zn
Base	Trace	< 0.001	0.01	< 0.002	< 0.005	< 0.005	0.01	Trace	0.01	0.02	< 0.01	< 0.01	< 0.01

history and its distribution in work piece during the welding process [9]. The importance of the issue is of two fold: first, we can determine whether welding is possible or not in a particular condition. Second, the thermal history and its distribution in a piece affect the residual stress and grain size, thus it affects the weld strength [9]. Hence, a lot of researchers have attempted to provide experimental strategies or analytical models to determine thermal distribution in the work piece [9]. For example, Hwang et al. could specify the thermal history in the specific parts of workpiece through placing thermometers in aluminum sheets and welding them using the mentioned method [9]. Also, Xue et al. evaluated the thermal effect on the mechanical properties of obtained welds via FSW on copper in water and air and at different temperatures; the maximum temperature was also determined [10]. Fujii et al. specified the thermal history on the underside of the steel sheets connected by friction stir method by putting thermometers on the welding boundary line [11]. Imam et al. compared the relationship between mechanical and microstructural properties of stir and heat affected zones of aluminum alloys using temperature monitoring [12].

Along with the conducted analytical and experimental studies, several numerical methods were developed for determining the field of thermal distribution and its history in some parts of work pieces. For instance, using DEFORM-3D software, Buffa et al. could specify the thermal field in two parts of AA6060-T4 aluminum pieces connected by FSW [13]. Moreover, using Euler model, Jacquin et al. determined the thermal history and distribution in AA6060-T4 aluminum sheets and then compared them with values obtained from the test [14]. Al-Badour et al. achieved the values of maximum temperature in FSW of AL6061-T6 aluminum through presenting Eulerian Lagrangian model and compared them with experimental values [15]. Darvazi et al. determined thermal history and field for some specific parts of steel sheets and compared them with experimental results [16].

In the present study, two copper pieces were welded together by the friction stir method under different welding conditions; the thermal history was also determined experimentally in specific parts of these pieces. Additionally, using numerical method and LS-Dyna software, the thermal history was determined at the same parts under the same circumstances and the obtained results were compared with experimental results.

## 2. Experiments

The material used in the study was copper. In terms of the weight percentage of its constituent elements, the chemical composition of the mentioned material is based on Table 1.

To perform the test, copper sheets were cut at dimensions of  $5 \times 50 \times 135\text{mm}^3$  and carefully sanded and polished so that after putting them together, no air would be trapped between them to weaken the weld. Then, sheets were longitudinally placed mutually side by side and by the help of the die used in the experiment, were quite stable to each other. Fig. 1 shows a portrait of the primary samples and samples of given weld with the conditions mentioned in Table 2. Also, the part whose temperature has experimentally and numerically been measured for each welding mode has been indicated in the Fig. 1(a). A view of the die and pieces fixed is given in Fig. 2. Also Fig. 2(b) shows how the samples were put in the die.

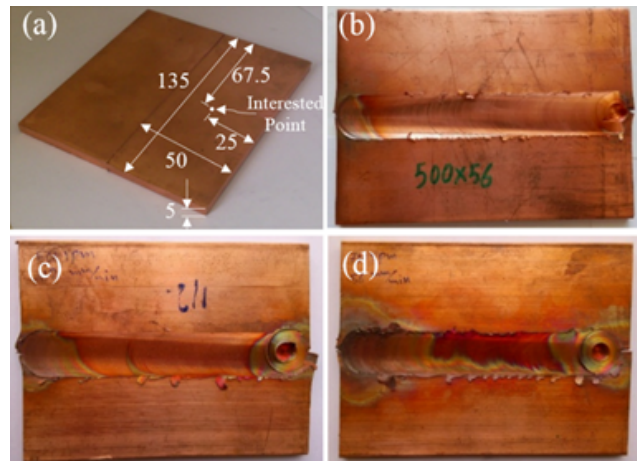


**Fig. 1.** a) The primary samples, b) Welded piece according to the first conditions on Table 2, c) Welded piece according to the second conditions on Table 2, d) Welded piece according to the third conditions on Table 2.

As it is known, the process of friction stir and the movement of rotary tool in the base material make its grain size and as a result, improve its mechanical properties. However, the heat transferred to the base material causes the grain growth. Therefore, it is always tried to do the process of friction stir welding at low temperature which has also been mentioned in almost all articles and references on the issue [11,17]. This shows the high importance of cooling during the process of friction stir. Accordingly, the die equipped with the cooling system was used in the study.

**Table 2**

Table of specific heat capacity and thermal conductivity coefficient of copper at various temperatures [22].

Investigated cases	Rotational speed, N (rpm)	Traverse speed, v (mm/min)
Case 1	500	56
Case 2	500	112
Case 3	710	56

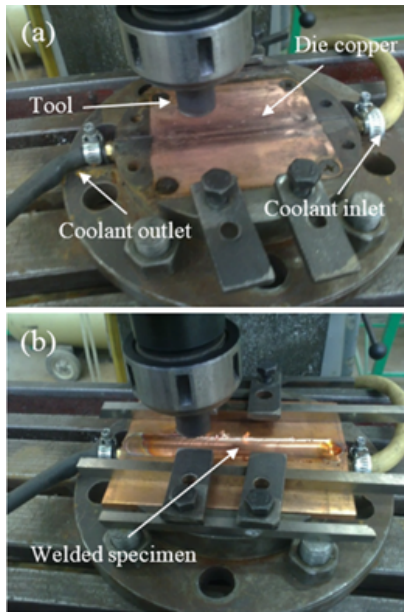


**Fig. 2.** a) A view of the used die and tools, b) Pieces trussed in the die after doing the process.

In order to do the process of cooling, a piece of copper having dimensions of  $100 \times 100 \times 10\text{mm}^3$  with two rather large grooves having the dimensions of  $100 \times 30 \times 6\text{mm}^3$  was installed at the bottom of the dies. Accordingly, the cooling water can pass with mass rate of  $\dot{m} = 0.019\text{kg/s}$  into the die. Die and copper sheet are shown in Fig. 2(a). These two grooves are beneath the copper sheet of the die and water enters into the die through two hoses as shown in Fig. 2(a) and exits from it. Copper was chosen for the bottom of the die because of its high thermal conductivity.

Rotary tool used for conducting FSW process includes a shoulder with a diameter of 20mm and a pin with a diameter of 8mm and length of 4.7mm. In order to improve the material travels, some threads were created on the pin which letting the material move better around the instrument and to some extent it will move the axis. This tool is shown in Fig. 3. Tilt angle was considered to be 2.5 degrees.

In order to investigate the thermal history and field in various modes, copper sheets were welded to each other under different welding parameters. So, by welding in different cases and using trial and error method, suitable welding parameters for successful welds on the aforementioned samples were determined. If the rotational speed and the traverse velocity are shown by N

and v, the mentioned conditions can be summarized according to Table 2.

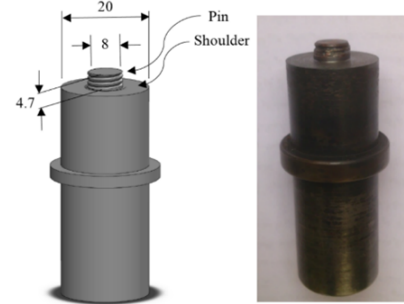


**Fig. 3.** Used tools (dimensions in mm).

An infra-red thermometer was used to measure the temperature in work piece. The thermometer was fixed on the table of milling machine and moves with it (Fig. 4). The thermometer temperature reads the thermal values for a particular point at any time and instantaneously sends the obtained information to a manual computer to record via a receiver. So, by focusing the thermometer on specific point of the surface of the workpiece, its thermal history can be recorded instantaneously on the computer. This particular point is the midpoint of one of the two sheets that should be welded together. This midpoint is part of the upper surface of the sheet way from the center of weld line with the size of 25mm and the end of the work piece with the size of 67.5mm.



**Fig. 4.** Thermometer installed on the table of angle grinder for measuring instantaneous temperature.

Here, it should be noted that in the process of FSW, the direction of the rotary tool on which the rotation of the tool is in the same direction with its movement is called advancing side and the rotation of the tool on the opposite direction with its movement is called retreading side. It should be noted that the part on which the thermometer was focused and thermal history was recorded was on the advancing side in all modes examined in the study.

In order to determine stress-strain diagram for the base metal at various temperatures, the standard samples of tensile test were prepared based on ASTM-E8 standard as shown in Fig. 5. The true stress-strain diagram from tensile test was obtained at two temperatures of 700°K and 800°K. These temperatures were chosen because they were approximately maximum that work pieces experienced on the modes mentioned in Table 2. These temperatures were measured by infra-red thermometer exclusively behind the tool in each welding mode.

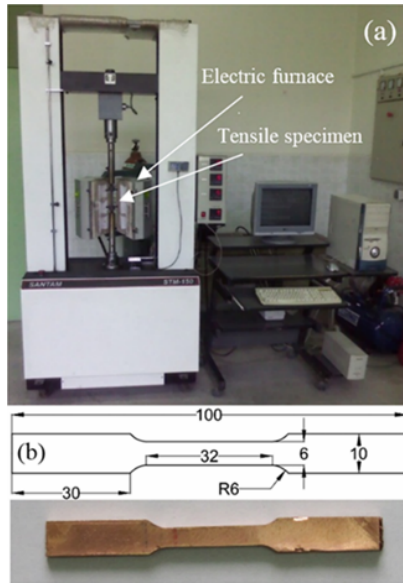


**Fig. 5.** a) Tensile testing machine and furnace installed on it b) Standard samples of tensile test.

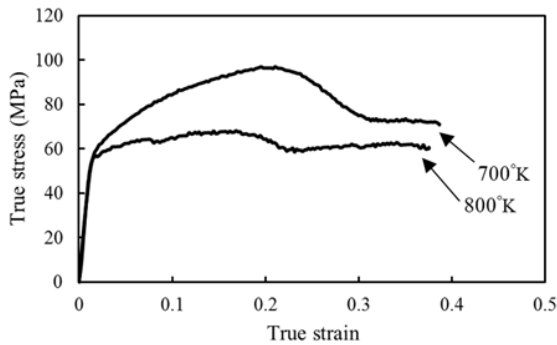


**Fig. 6.** True stress-strain diagram of the base metal at various temperatures.

### 3. Simulations

In order to simulate and determine the thermal field numerically in work piece, LS-Dyna software was used. For modeling the process of welding in the software, the option of thermal weld was used. This was particularly included to simulate the process of welding in the mentioned software. Using this option, the rotary tool that is the thermal generator in the process of fric-

tion stir can be modeled as a heat source and moved along the surface of work piece with the desired speed. By moving this heat source on the work piece, the heat is transferred to the work piece and the temperature of the work piece increases at various parts based on the heat transfer rate.

To determine the produced heat rate within the process of friction stir by the rotary tool, relations presented in various references for this purpose can be used. One of these relations is the one provided by Frigadd et al. [18] and was used for calculating the heat generated by the tool. This relation is as follows:

$$\dot{q} = \frac{4}{3}\pi^2\mu PwR^3 \quad (1)$$

Where  $q$ ,  $\mu$ ,  $P$ ,  $w$  and  $R$  are the rate of net heat input (W), the coefficient of dynamic friction, pressure (Pa), the angular speed (rps) and tool radius (m), respectively. According to Frigadd, the rotational speed of tool and its radius have the greatest effect in the relation. Moreover, Frigadd et al. [18] suggested that the rate of “P” can be considered equal to flow stress at the temperature of the process [18]. In order to measure the validity of the mentioned relation, some sheets were with different aluminum materials and subsequently the process of FSW was conducted on them. Frigadd et al. experimentally obtained the temperature by placing thermometers in samples. Then the results were compared with the above relation. By performing this test, it was found that there is a good agreement between the experimental results and those obtained from the relation [18]. After Frigadd, other researchers such as Chao and Qi [18] and Khandkar and Khan [18] confirmed the validity of the relation suggested by Frigadd through tests on other materials.

In the preset study, to obtain the rate of produced net heat, the above relation was used. In so doing, the dynamic friction coefficient between tool and work piece was considered equal to 0.36 [19].  $P$ -Value was equal to the flow stress for the material of work piece at the considered temperature according to the diagrams given in Fig. 6. As we know, the flow stress is the stress under which the material stress suffers from plastic deformation. As given in Fig. 6, it can be found that after crossing the yield stress and entering to the flow area, the true stress-strain diagram of copper at high temperature becomes first ascending and then descending and there after, it will be horizontally and fairly constant in a way that the more the temperature is high, the more the rate of ascending and descending will decrease and the longer horizontal part of the diagram will be. Therefore, using Eq. (1) and obtaining the rate of produced heat at the clear temperature and a specified rotation of tool (N), a constant number should be used and this number, i.e. the flow stress of work piece material was considered as the stress of horizontal part of stress-strain curve in Fig. 6. Thus,

$P$  was considered at the temperature of 700°K equal to 72MPa and 800°K equal to 61MPa.

According to what was said, to calculate the rate of transferred heat at the rotation of 500 rpm using Eq. (1), it can be written:

$$\begin{aligned}\dot{q} &= \frac{4}{3}\pi^2\mu PwR^3 \quad (2) \\ &= \frac{4}{3}\pi^2(0.36)(72 \times 10^6 Pa) \left(\frac{500}{60} rps\right) (10 \times 10^{-3} m)^3 \\ &= 2842.45W\end{aligned}$$

Also, to calculate the rate of transferred heat at the rotation of 710rpm using Eq. (1), we have:

$$\begin{aligned}\dot{q} &= \frac{4}{3}\pi^2(0.36)(61 \times 10^6 Pa) \left(\frac{710}{60} rps\right) (10 \times 10^{-3} m)^3 \\ &= 3419.62W \quad (3)\end{aligned}$$

To consider boundary conditions, it was assumed that 10% of the heat created by the tool is wasted through the tool itself and the thermal conductivity [20]. Therefore, it was assumed that 90% of the heat created by the tool is spent to do the process. So, for the two above-mentioned states, the net heat transferred to the work piece cases at the rotation speed of 500rpm could be written:

$$\dot{q}_{net} = 0.9 \times 2842.45W = 2558.2W \quad (4)$$

At the rotation of 710 rpm:

$$\dot{q}_{net} = 0.9 \times 3419.62W = 3077.65W \quad (5)$$

It was also assumed that water with the ambient temperature passes through two channels of copper sheet and exchanges the heat through (convective) transmission with the copper sheet and as a result, work piece. All cases of heat exchange during the heat transfer are negligible and can be ignored; for example, the rate of transferred heat by the work piece to air or small components of the die.

If the specific heat capacity of water is considered as  $c = 4200J/kg \cdot ^\circ K$  [21], to obtain the outlet water temperature of the format, we can write:

At the rotation of 500rpm:

$$\begin{aligned}\dot{q}_{net} &= \dot{m}c\Delta T \implies \\ 2558.2W &= 0.019kg/s \times 4200J/kg \cdot ^\circ K \times \Delta T \quad (6) \\ \implies \Delta T &= 32^\circ K\end{aligned}$$

At the rotation of 710 rpm:

$$\begin{aligned}3077.65W &= 0.019kg/s \times 4200J/kg \cdot ^\circ K \times \Delta T \\ \implies \Delta T &= 38.6^\circ K \quad (7)\end{aligned}$$

The water temperature at the inlet to the die was 298°K. Therefore, the water temperature at the outlet

would be 330°K at the rotation of 500rpm and 336.6°K at the rotation of 710rpm. To perform the simulation, the average temperature of the inlet and outlet was considered as cooling water temperature, i.e. temperatures of 314°K and 317.3°K can be regarded for rotations of 500rpm and 710rpm respectively.

To calculate the convective heat transfer coefficient ( $h$ ), the relation of convective heat transfer was used:

$$\dot{q}' = Ah\Delta T \quad (8)$$

In the above relation,  $q$  is the rate of heat transferred to the cooling water (W) and  $A$  is the area of the format channel moistened by water. So it is as below:

$$A = 2 \times [(6 + 30 + 6) \times 100]mm^2 = 8.4 \times 10^{-3}m^2 \quad (9)$$

Now, given that the heat that the copper sheet at the bottom of die takes from work piece is directly transferred to cooling water, we have:

$$\begin{aligned}\dot{q}' = \dot{q} &\implies Ah\Delta T = \dot{m}c\Delta T \\ \implies h &= \frac{\dot{m}c}{A} = \frac{0.019kg/s \times 4200/kg \cdot ^\circ K}{8.4 \times 10^{-3}m^2} \quad (10) \\ &= 9500W/m^2 \cdot ^\circ K\end{aligned}$$

However, it should be noted that  $h$  coefficient is not often a constant value and depends on parameters such as the length of the pipe (channel), Nusselt number, etc., but the value obtained from the above relation can be accepted as average  $h$  in the channel.

Given that the specific heat capacity and thermal conductivity coefficient of copper have different values at various temperatures, these two quantities were introduced to software in terms of temperature and according to Table 3 [22].

In order to approximate the simulations to the conducted experiments, thermal source (welding tool) was considered as a fixed point in space and right above the two half of work piece and at the beginning of the weld line. In fact, two halves of work piece are passed under the thermal source with constant speed. Each half of work piece was classified by 2700 cubic elements. As it was explained in the section of experiments, two halves work pieces with copper sheets at the bottom of the die play a significant role in heat exchange, so the exchange should be considered in the simulation. Therefore, copper sheet of the die and two water passing channels were modeled with the help of 2800 cubic elements. Given that the work piece became practically tight on the copper sheet of the die by the die constraints and completely contacted with it at any moment, classifying the elements of work pieces and copper sheet was done in the way that nodes of elements overlapped at their common surface and then, nodes consistent with each other were connected desirably do the heat exchange between two halves of the

work pieces and copper sheet of the die. So, the number of elements is totally 8200 and the number of nodes is 11572. Fig. 7 shows an image of full model.

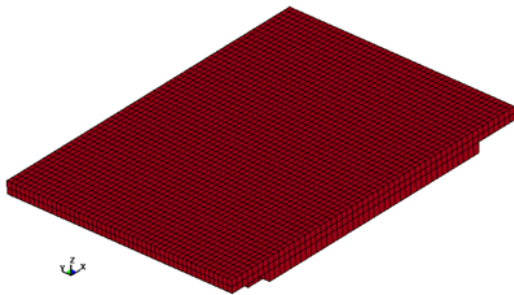


Fig. 7. An image of full simulation model.

Table 3

Table of specific heat capacity and thermal conductivity coefficient of copper at various temperatures [22].

Temperature (°K)	Thermal conductivity (W/m°K)	Heat capacity (J/Kg°K)
200	412	343
350	396	391
500	387	403
650	376	425
800	365	437
950	355	455
1100	345	468
1250	334	478

So, there is no need to define the contact between various components of the issue. In this simulation, due to its high accuracy, the model of piece wise linear plasticity material was used. Using this model, the parts of stress-strain diagram of the material are identically presented to the software without need for the curve fitting. The copper density was considered equal to  $8900 \text{ kg/m}^3$  and the initial temperature of all components equal to  $298^\circ\text{K}$ . The boundary conditions of this simulation were also the heat conductive exchange with welding tools and the heat velocity exchange with cooling water.

Through simulations, the thermal field could be

easily achieved at any time and for any welding mode. Fig. 8 shows the thermal field in three different welding modes and when welding tool is located in the middle of the sheet. Also, Fig 9(a) indicates the thermal history for a part of work pieces whose thermal history was experimentally measured and Fig. 9(b) reveals the thermal history for the part which the heat source passes on and places in the middle of the intersection line of two pieces. In order to compare the experimental results with simulation results, the diagrams of the thermal history of each methods were obtained in various modes mentioned in Table 2 and compared with each other.

#### 4. Results and Discussion

According to Fig. 9, it is evident that the effect of rotational speed of tool on the maximum rate of temperature is much more than the effect of its traverse-velocity. Fig. 9(b) reveals that 100% increase in the traverse velocity from  $56\text{mm/min}$  to  $112\text{mm/min}$  has led to decrease in the maximum temperature from  $715^\circ\text{K}$  to  $693^\circ\text{K}$  which is by no means a significant value. If the rotational speed increases from  $500\text{rpm}$  to  $710\text{rpm}$ , accordingly 24-percentage, then the maximum temperature will increase from  $715^\circ\text{K}$  to  $802^\circ\text{K}$ . Furthermore, according to diagrams in Fig. 9, it can be seen that although increasing the traverse velocity has no little effect on the thermal rate experienced in the desired parts, it causes that each part experiences the related temperature at less duration, i.e. transferring less heat. Moreover, according to Fig. 9(a), it can be understood that by increasing the rotational speed of the tool, the considered parts of work piece bear more temperature and an increase in the temperature is visible. Therefore, in summary, it can be said that the traverse velocity change mainly affects the transferred heat rate and the change in the rotational speed dramatically changes the temperature of the process.

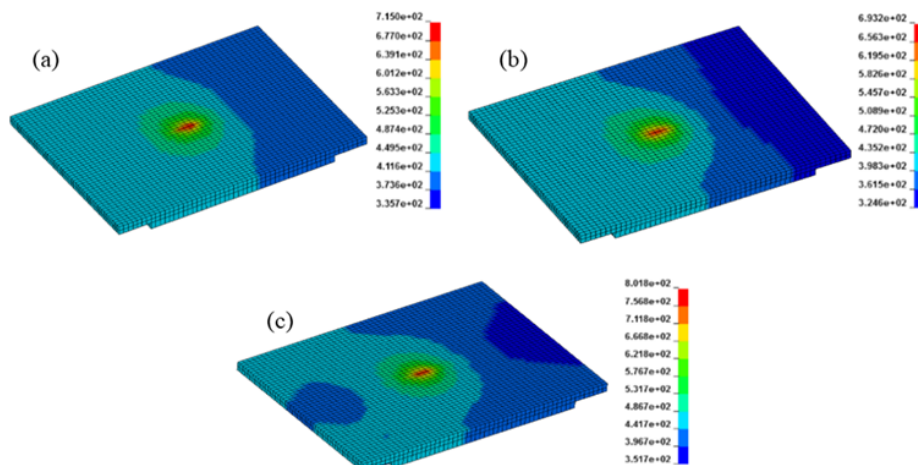


**Fig. 8.** Thermal field in three different modes (according to Table 2) of welding: a) Mode 1, b) Mode 2 and c) Mode 3.

In Fig. 10, the thermal diagrams obtained from the experiment and simulation are compared with each other. According to these diagrams, it can be found that the simulation diagrams are lower than the diagrams obtained from the experiment because the estimated heat rate is slightly less than the true heat rate. This is because in estimating the heat rate, flow stress was considered to be equal to the flow stress of horizontal part of the diagram; the overall flow stress is slightly higher than this value. However, in large strains which occur in the friction stir process, this part of the diagram is not quite noticeable; over time, the trend in the process of diagrams from the simulation and experiment is reversed and the diagrams from simulation are placed higher because of the effect of ignored heat loss.

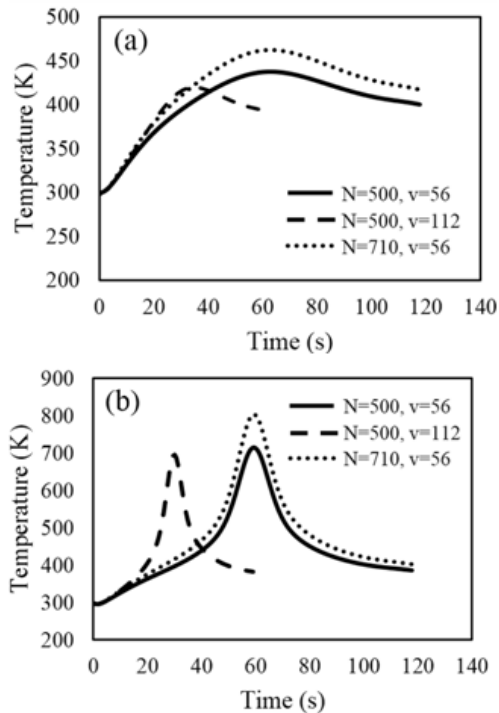


**Fig. 9.** a) The thermal history in the part of work pieces whose thermal history was experimentally measured and b) The thermal history in the part on which the heat source passes and places in the middle of the intersection line of two pieces (N(rpm), v(mm/min)).

Over time, their value in experiment will increase while there is no loss in simulation. But in general, what is important is that values of these differences are not significant compared to temperatures on which the process is done and with a little ignorance, the obtained diagrams can be considered to be coincided. This suggests that it can predict the thermal history and field only by doing a tension test on samples prepared from the desired material and using LS-Dyna software and

its thermal weld option. So, it is clear that using the advantages of the numerical method, it can save time and cost along with correctly predicting the thermal field at any moment in work pieces regarding that the complex pieces have no need to be welded.

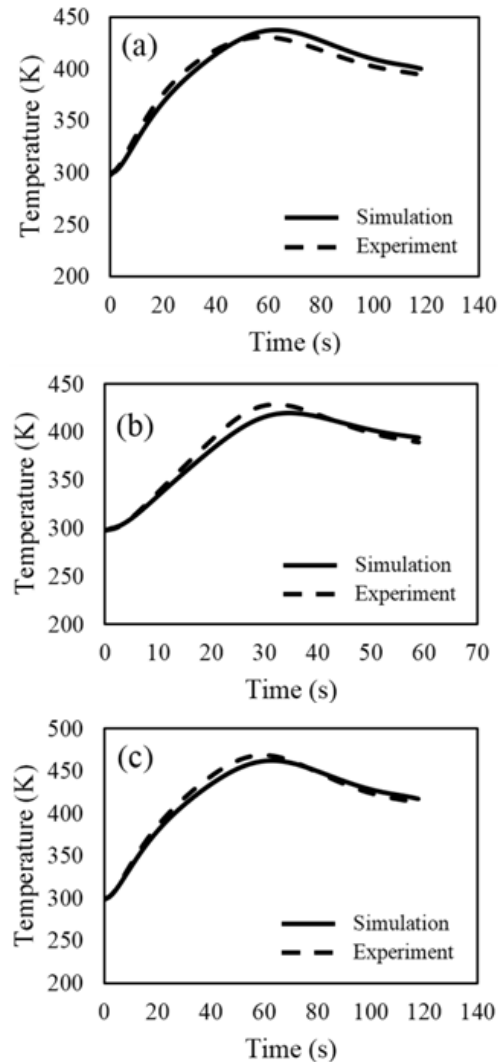


**Fig. 10.** Comparing the experimental and simulation results (a) First mode; (b) Second mode and (c) Third mode.

In addition, this study shows that the relation proposed by Frigadd et al. has been successful to estimate the rate of heat transferred to the work piece within FSW, thus the relation is valid for the copper work piece.

It is worth mentioning that in some studies, it has been attempted to completely simulate the process of friction stir with the help of finite element methods and meshing of pieces and predict the proper motion of material which is a three-dimensional motion [22,23]. While given that in the process deformations

are very large, elements will be much distorted so that the success of this method seems unlikely even using remeshing. In this regard, using meshless methods such as SPH is not helpful because in these cases, there is no surface due to no mesh, therefore no heat is created as an effect of friction and any heat can transfer from the surface of work piece and thus, the process of heat transferred to the die or cooling process cannot be stimulated. However, to perform simulations better than what was done in this study, it is suggested using either software designed for large deformations such as Comsol. Paying attention to occurrence of large deformation and fluid-like movement of material that is located around the welding tool, the welded material can be assumed as a fluid and a software in the field of fluid mechanics, can be used.

## 5. Conclusions

In this study, the thermal histories in copper sheets were determined experimentally and numerically during a Friction Stir Welding butt joining process and were compared with each other. The following conclusions can be drawn based on the results:

1. The selected welding conditions, rotational speeds of 500 and 710rpm and traverse velocities of 56 and 112mm/min, are appropriate conditions and result in obtaining desirable welds.
2. The traverse velocity change mainly affects the transferred heat rate and the change in the rotational speed dramatically change the temperature of the process. For example 100% increase in the traverse velocity from 56 to 112mm/min has led to decrease in the maximum temperature from 715 to 693°K which is by no means a significant value, while the rotational speed increases from 500 to 710 rpm, accordingly 24-percentage, then the maximum temperature will increase from 715 to 802°K.
3. The relation proposed by Frigadd et al. has been successful to estimate the rate of heat transferred to the work piece within FSW, thus the relation is valid for the copper work piece.
4. It is possible to predict the thermal history and field successfully, only by doing a tension test on samples prepared from the desired material and using LS-Dyna software and its thermal weld option.

## References

[1] Y.F. Sun, H. Fujii, The effect of SiC particles on the microstructure and mechanical properties of friction

stir welded pure copper joints, *Mater. Sci. Eng. A*, 528 (2011) 5470-5475.

- [2] A. Bagheri, T. Azdast, A. Doniavi, An experimental study on mechanical properties of friction stir welded ABS sheets, *Mater. Des.*, 43 (2013) 402-409.
- [3] M. Pirizadeh, T. Azdast, S. Rash Ahmadi, S. M. Shishavan, A. Bagheri, Friction stir welding of thermoplastics using a newly designed tool, *Mater. Des.*, 54 (2014) 342-347.
- [4] S. Khalilpourazary, R.A. Behnagh, R. Mahdavinjad, N. Payam, Dissimilar friction stir lap welding of Al-Mg to CuZn34: Application of grey relational analysis for optimizing process parameters, *J. Comput. Appl. Res. Mech. Eng.*, 4 (2014) 81-88.
- [5] X. Cao, M. Jahazi, Friction-stir welding of dissimilar AA 2024-T3 to AZ31B-H24 alloys, *Int. J. Adv. Manuf. Technol.*, 46 (2010) 1259-1259.
- [6] Y. Zhao, S. Jiang, S. Yang, Z. Lu, K. Yan, Influence of cooling conditions on joint properties and microstructures of aluminum and magnesium dissimilar alloys by friction stir welding, *Int. J. Adv. Manuf. Technol.*, 83 (2016) 673-679.
- [7] Z. Zhang, H.W. Zhang, A fully coupled thermo-mechanical model of friction stir welding, *Int. J. Adv. Manuf. Technol.*, 37 (2008) 279-293.
- [8] Y.F. Sun, H. Fujii, Investigation of the welding parameter dependent microstructure and mechanical properties of friction stir welded pure copper, *Mater. Sci. Eng. A.*, 527 (2010) 6879-6886.
- [9] Y.M. Hwang, Z.W. Kang, Y.C. Chiou, H.H. Hsu, Experimental study on temperature distributions within the work piece during friction stir welding of aluminum alloys, *Int. J. Mach. Tools Manuf.*, 48 (2008) 778-787.
- [10] P. Xue, B.Xiao, Q. Zhang, Z. Ma, Achieving friction stir welded pure copper joints with nearly equal strength to the parent metal via additional rapid cooling, *Scripta Mater.*, 64 (2011) 1051-1054.
- [11] H. Fujii, L. Cui, N. Tsuji, M. Maeda, K. Nakata, K. Nogi, Friction stir welding of carbon steels, *Mater. Sci. Eng. A.*, 429 (2006) 50-57.
- [12] M. Imam, K. Biswas, V. Racherla, On use of weld zone temperatures for online monitoring of weld quality in friction stir welding of naturally aged aluminium alloys, *Mater. Des.*, 52 (2013) 730-739.
- [13] G. Buffa, A. Ducato, L. Fratini, Numerical procedure for residual stresses prediction in friction stir welding, *Finite Element. Anal. Des.*, 47 (2011) 470-476.

- [14] D. Jacquin, B. De Meester, A. Simar, D. Deloison, F. Montheillet, C. Desrayaud, A simple Eulerian thermo mechanical modeling of friction stir welding, *J. Mater. Process. Technol.*, 211 (2011) 57-65.
- [15] F. Al-Badour, N. Merah, A. Shuaib, A. Bazoune, Coupled Eulerian Lagrangian finite element modeling of friction stir welding processes, *J. Mater. Process. Technol.*, 213 (2013) 1433-1439.
- [16] A.R. Darvazi, M. Iranmanesh, Prediction of asymmetric transient temperature and longitudinal residual stress in friction stir welding of 304L stainless steel, *Mater. Des.*, 55 (2014) 812-820.
- [17] P. Prasanna, B.S. Rao, G.K. Rao, Finite element modeling for maximum temperature in friction stir welding and its validation, *Int. J. Adv. Manuf. Technol.*, 51 (2010) 925-933.
- [18] A. Alavi Nia, H. Omidvar, S. Nourbakhsh, Investigation of the effects of thread pitch and water cooling action on the mechanical strength and microstructure of friction stir processed AZ31, *Mater. Des.*, 52 (2013) 615-620.
- [19] R.S. Mishra, Z. Ma, Friction stir welding and processing, *Mater. Sci. Eng. R: Reports*, 50 (2005) 1-78.
- [20] P.J. Blau, *Friction Science and Technology: From Concepts to Applications*, 2nd ed., Taylor & Francis, (2012).
- [21] L.Z. Jin, R. Sandström, Numerical simulation of residual stresses for friction stir welds in copper canisters, *J. Manuf. Process.*, 14 (2012) 71-81.
- [22] F.P. Incropera, T.L. Bergman, D.P. DeWitt, A.S. Lavine, *Foundations of Heat Transfer*, Wiley, Limited, (2013).
- [23] P. Ulysse, Three-dimensional modeling of the friction stir-welding process, *Int. J. Mach. Tools Manuf.*, 42 (2002) 1549-1557.
- [24] J. Hilgert, H.N.B. Schmidt, J.F. Dos Santos, N. Huber, Thermal models for bobbin tool friction stir welding, *J. Mater. Process. Technol.*, 211 (2011) 197-204.